Supporting information

Fluorescence properties of novel deep-red phosphor $LiMg_4SbO_7:Mn^{4+}$ with excellent quantum efficiency and color purity for warm white LEDs

Fei Wang[‡ *a,c,d], Huihui Chen[‡b], Shiwei Zhang[*a,c], Huiqing Jin[*a,c]

[a]*Key Laboratory of Traffic Information and Safety of Anhui Higher Education Institutes, Anhui Sanlian University, Hefei 230601, People's Republic of China*

[b]*Department of Pharmacy, the 901th Hospital of the Joint Logistics Support Force of People's Liberation Army, Hefei,230031,People's Republic of China*

[c]*Anhui Sanlian Group, Hefei 230601, People's Republic of China*

[d]*Department of Chemistry, Anhui University, Hefei 230601, China*

‡These authors contributed equally to this work and should be considered co-first authors.

**Corresponding author: wangfchina@163.com; jinhuiqing@slu.edu.cn*

Experiment

Samples synthesis

The amount of each target samples $LiMg_4Sb_{1-x}O_7$:$x$$Mn^{4+}$($0.001 \le x \le 0.006$, Δx=0.001) synthesized is 0.0150 mol, and the exact mass of each synthetic raw material is weighed as follows, taking the sample of $LiMg_4SbO_7$:0.002Mn^{4+} (x=0.002) as an example, 0.5542 g (0.0075 mol) Li_2CO_3 (AR, Aladdin), 5.8296 g (0.0120 mol) $(MgCO_3)_4 \cdot Mg(OH)_2 \cdot 5H_2O$ (AR, Aladdin), 2.4215 g (0.0075 mol) Sb_2O_5 (99%, Aladdin), 0.0035 g (0.00003 mol) $MnCO_3$ (99.95%, Aladdin) and the mass of co-solvent H_3BO_3(GR) is 6% of the total mass of all raw materials, which is 0.5285 g.

Sample synthesis conditions: (1) Heating rate: 15℃/min, (2) Cooling method: natural cooling to room temperature with the furnace

Instrument parameters

The diffraction data of each sample was collected by the D8 Advance X-ray powder diffractometer (Germany, Bruker). Instrument parameters: the radiation source was Cu target, Kα1 radiation λ=0.15406 nm, 40 mA, 40 kV, divergent slit 1 mm, receiving slit 0.1 mm, anti-scatter slit 1 mm. Step scanning, step speed: 5 $sec \cdot step^{-1}$, step size: 0.01 °, scanning range 10-60 °, using standard α-Al_2O_3 to correct the diffraction peak.

The sample morphology was examined by scanning electron microscopy (SEM, Germany, Zeiss Sigma 300) and the elemental composition was analyzed by energy dispersive X-ray spectrometry (EDX). Instrument parameters: Model of energy spectrometer: Smart EDX; Gold spraying target: pure gold; Electron Gun: Schottky Field Emission Electron Gun; Resolution: 1.0nm@15kV, 1.6nm@1kV; Electron light path: There is no cross light path for electron beams in the lens barrel; Accelerating voltage: 0.02-30kV, continuously adjustable in 10V steps; Probe beam current: 3pA-20nA, stability better than 0.2%/h; Magnification: 10x -1,000,000x; Objective: Electromagnetic/Electrostatic Compound Lens; Detectors: Inlens and ET secondary electron detectors, and EDS spectrometers; Spectrum model: Smartedx; Energy spectrum analysis working distance: 8.5 mm; Sample Chamber Dimensions: 365mm x 275mm; Stage travel: X = 125mm; Y = 125mm; Z = 50mm; T = -10°to 90°; R = 360° (continuously adjustable); Image capture: up to 32k x 24k.

X-ray photoelectron spectroscopy (XPS) of the samples obtained with Thermo Scientific K-Alpha (USA) (Excitation source: Al Kα rays (hv=1486.6eV); Beam spot: 400um; Analysis chamber vacuum better than 5.0E-7m Bar; Working voltage: 12kV; Filament current: 6 mA; Full spectrum scan: step size 1eV;Narrow spectrum scan: step size 0.05 eV).

Fluorescence spectrometer type: UK, Edinburgh FS5, Excitation light source: Xenon lamp, Scanning speed: 1 $nm\cdot s^{-1}$, Excitation slit width: 0.8, Emission slit width：0.4.

Photoluminescence quantum efficiency is defined as the ratio of the emitted photons to the absorbed photons, and was measured by a spectrofluoremeter (UK, Edinburgh, FLS1000). An integrating sphere was mounted on the spectrofluoremeter with the entrance and exit ports located in 90^{o} geometry. The PiG sample was located in the center of the integrating sphere. All the recorded spectroscopic data were corrected for the spectral responses of both the spectrofluoremeter and the integrating sphere. The responses of the detecting systems (integrating sphere, monochromators and detectors) in photon flux were determined using a calibrated tungsten lamp. Based on this setup, The internal quantum efficiency (IQE) and external quantum efficiency (EQE) are calculated using the following formulas, respectively:

$$IQE = \frac{Number\ of\ photons\ emitted}{Number\ of\ photons\ absorbed} = \frac{L_{sample}}{E_{reference} - E_{sample}} \qquad (1)$$

$$EQE = \frac{Number\ of\ photons\ emitted}{Number\ of\ photons\ absorbed} = \frac{L_{sample}}{E_{reference}} \qquad (2)$$

L_{sample} the emission intensity, $E_{reference}$ and E_{sample} the intensities of the excitation light not absorbed by the reference and the sample respectively. The precursor glass was used as the standard reference. The difference in integrated areas between the sample and the reference represents the number of the absorbed photons. The photons emitted were determined by integrating the area of the emission band.

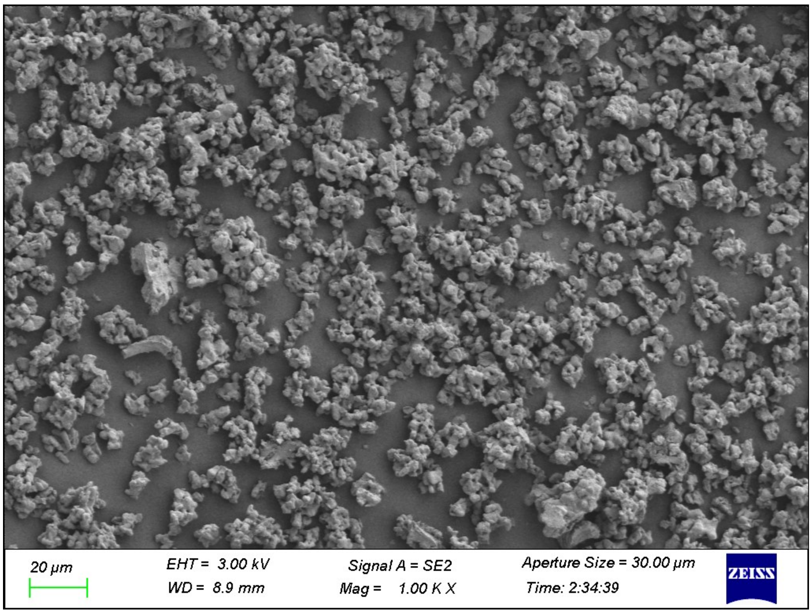

Fig. S1. The SEM image of $LiMg_4SbO_7$:0.002Mn^{4+} (20 μm)

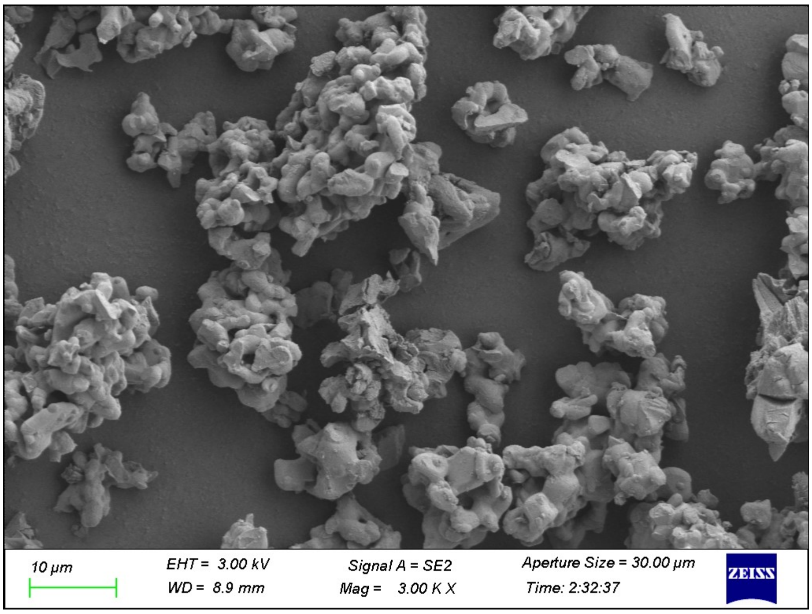

Fig. S2. The SEM image of $LiMg_4SbO_7$:0.002Mn^{4+} (10 μm)

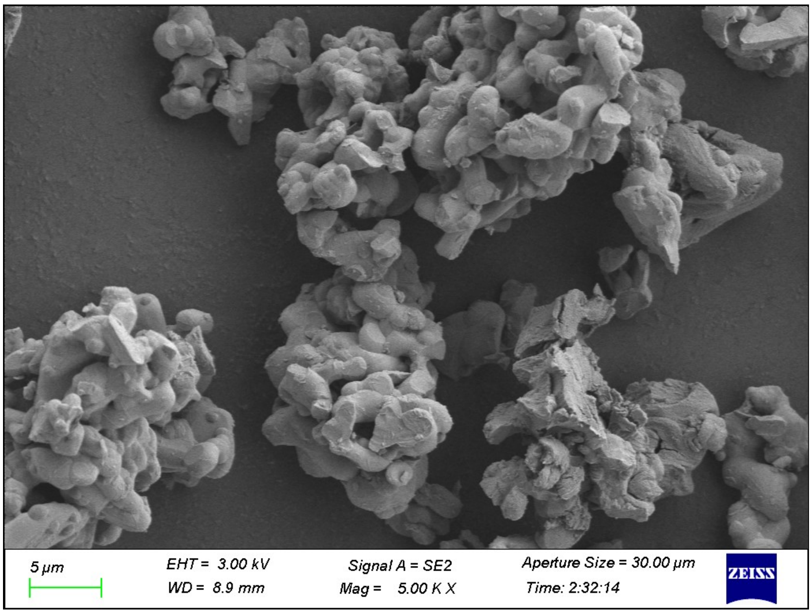

Fig. S3. The SEM image of $LiMg_4SbO_7$:0.002Mn^{4+} (5 μm)

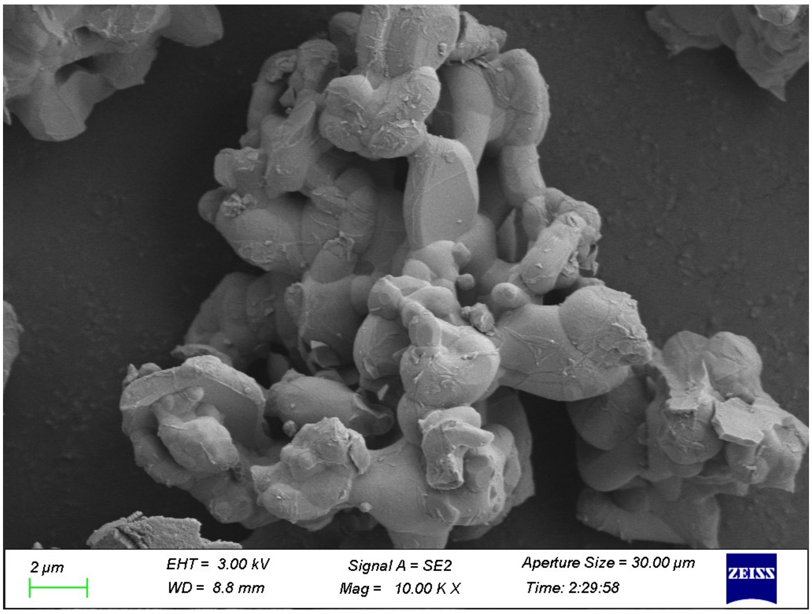

Fig. S4. The SEM image of $LiMg_4SbO_7$:0.002Mn^{4+} (2 μm)

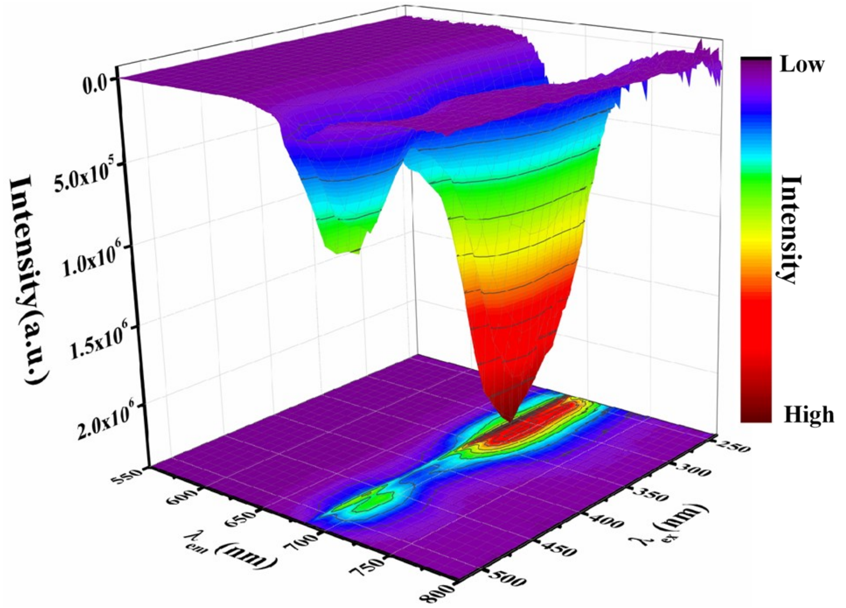

Fig. S5. Emission spectra and emission spectrum energy distribution of $LiMg_4SbO_7$:0.002Mn^{4+} under different excitation wavelengths (λ_{ex}=240-520 nm, 10nm)

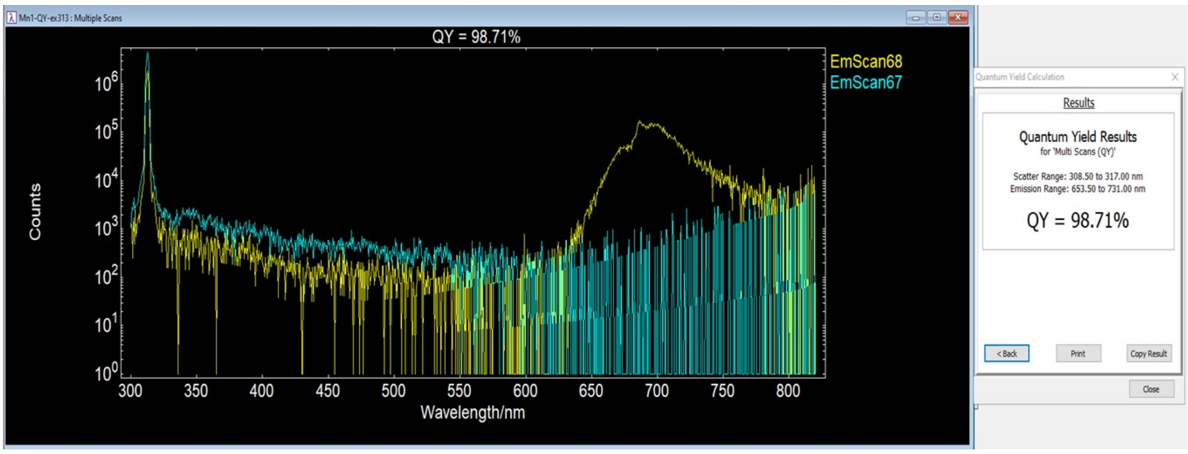

Fig.S6 The IQE curve of $LiMg_4SbO_7$:0.002Mn^{4+} phosphor (λ_{ex} = 313 nm)

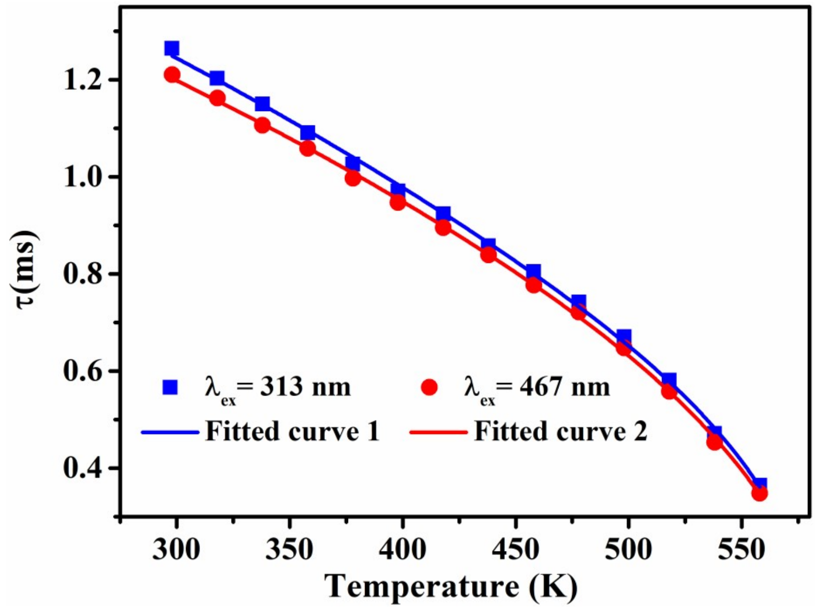

Fig.S7 Temperature-dependent average lifetime of $LiMg_4SbO_7$:0.002Mn^{4+}

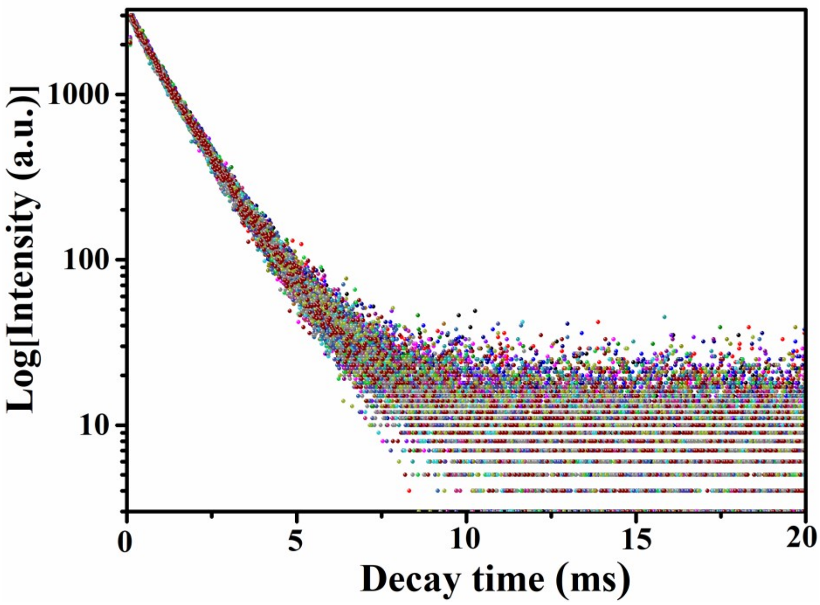

Fig. S8 The decay curves of $LiMg_4SbO_7$:0.002Mn^{4+} in 30 measurements (λ_{ex}= 313 nm, λ_{em}= 686 nm)

Table S1. Decay properties of $LiMg_4SbO_7$:$x$$Mn^{4+}$ (0.001≤x≤0.006) (λ_{ex}=313 nm, λ_{em}=686 nm).

Eu content (x)	A_1	A_2	τ_1 (ms)	τ_2 (ms)	τ (ms)	χ^2	Fitted function
x=0.001	2207.16	524.30	1.0928	2.0412	1.3838	1.4369	Double exponential

x=0.002	2208.63	2583.34	0.9076	1.4547	1.2644	1.1439	Double exponential
x=0.003	1190.44	1640.48	0.5986	1.3382	1.1570	1.0750	Double exponential
x=0.004	957.88	1831.42	0.2606	1.1104	1.0175	1.3905	Double exponential
x=0.005	1297.92	1185.31	0.4785	1.2313	1.0066	1.5561	Double exponential
x=0.006	1252.89	1536.46	0.1855	0.9480	0.8431	1.5840	Double exponential

Table S2. Decay properties of $LiMg_4SbO_7$:0.002Mn^{4+} phosphor at different test temperatures (λ_{ex}=313 nm, λ_{em}=686 nm).

Temperature	A_1	A_2	τ_1 (ms)	τ_2 (ms)	τ (ms)	χ^2	Fitted function
298 K	2208.63	2583.34	0.9076	1.4547	1.2644	1.1439	Double exponential
318 K	2946.73	1932.70	0.9346	1.4640	1.2029	1.2652	Double exponential
338 K	2235.81	2506.77	0.7977	1.3372	1.1499	1.3731	Double exponential
358 K	2445.72	2508.86	0.7616	1.2810	1.0905	1.3106	Double exponential
378 K	1643.43	3158.71	0.6118	1.1413	1.0258	1.2683	Double exponential
398 K	1742.01	2997.79	0.5848	1.0909	0.9707	1.3142	Double exponential
418 K	2017.75	2720.37	0.5812	1.0625	0.9236	1.3099	Double exponential
438 K	1880.58	3062.20	0.4743	0.9724	0.8576	1.2299	Double exponential
458 K	1981.36	2816.23	0.4376	0.9264	0.8045	1.4290	Double exponential
478 K	2506.62	2172.74	0.4394	0.9106	0.7421	1.4659	Double exponential
498 K	2219.55	2452.36	0.3578	0.7979	0.6708	1.5113	Double exponential
518 K	2291.03	2367.97	0.3020	0.6980	0.5811	1.6903	Double exponential
538 K	2672.36	1998.09	0.2774	0.5925	0.4712	1.7901	Double exponential
558 K	2933.08	1474.86	0.2247	0.4918	0.3647	1.8163	Double exponential

Table S3. Decay properties of $LiMg_4SbO_7$:0.002Mn^{4+} phosphor at different test temperatures (λ_{ex}=467 nm, λ_{em}=686 nm).

Temperature	A_1	A_2	τ_1 (ms)	τ_2 (ms)	τ (ms)	χ^2	Fitted function
298 K	1917.18	2971.08	0.8041	1.3652	1.2107	1.3942	Double exponential
318 K	1252.96	3756.34	0.6174	1.2523	1.1626	1.3941	Double exponential
338 K	2911.77	1891.73	0.8417	1.3590	1.1065	1.4510	Double exponential
358 K	1911.07	2838.77	0.6673	1.2048	1.0588	1.7147	Double exponential
378 K	1885.72	2728.59	0.6322	1.1369	0.9968	1.5202	Double exponential
398 K	2524.69	2272.71	0.6538	1.1347	0.9470	1.7033	Double exponential
418 K	2639.38	2249.74	0.6205	1.0806	0.8954	1.7466	Double exponential
438 K	2495.53	2307.33	0.5547	1.0083	0.8391	1.7502	Double exponential
458 K	1881.44	2799.56	0.4004	0.8908	0.7771	1.8181	Double exponential
478 K	2219.76	2613.74	0.3853	0.8507	0.7214	1.8732	Double exponential
498 K	2363.05	2401.29	0.3409	0.7796	0.6476	1.8623	Double exponential
518 K	2407.20	2535.49	0.2759	0.6686	0.5581	1.8155	Double exponential
538 K	2227.00	2543.69	0.2135	0.5364	0.4530	1.8279	Double exponential
558 K	1781.76	1195.12	0.2048	0.4468	0.3486	1.8012	Double exponential

Table S4 Optoelectronic parameters of LED-3 under different current drives.

Current	CIE (x, y)	CCT	CRI	LE (lm/W)
10 mA	(0.3575, 0.3809)	4687 K	83.6	118.78
30 mA	(0.3560, 0.3762)	4713 K	83.8	118.00
50 mA	(0.3548, 0.3729)	4737 K	83.9	114.38
70 mA	(0.3537, 0.3701)	4761 K	84.0	110.73
90 mA	(0.3528, 0.3676)	4780 K	84.1	107.19
110 mA	(0.3518, 0.3652)	4804 K	84.2	103.86
130 mA	(0.3510, 0.3632)	4823 K	84.5	100.43
150 mA	(0.3502, 0.3614)	4844 K	84.5	96.80
170 mA	(0.3496, 0.3596)	4858 K	84.7	94.71
190 mA	(0.3488, 0.3577)	4879 K	84.8	92.23
210 mA	(0.3481, 0.3562)	4898 K	84.9	89.49
230 mA	(0.3474, 0.3545)	4917 K	85.1	87.01
250 mA	(0.3466, 0.3529)	4941 K	85.1	84.73

270 mA	(0.3460, 0.3514)	4958 K	85.4	82.20
290 mA	(0.3453, 0.3499)	4980 K	85.5	79.91